TREE OF SHAPES CUT FOR MATERIAL SEGMENTATION GUIDED BY A DESIGN

Julien Baderot[a], *Michel Desvignes*[a], *Laurent Condat*[a], *Mauro Dalla Mura*[a,b]

[a] Univ. Grenoble Alpes, CNRS, Grenoble INP*, GIPSA-lab, 38000 Grenoble, France
* Institute of Engineering Univ. Grenoble Alpes
[b] Tokyo Tech World Research Hub Initiative (WRHI), School of Computing,
Tokyo Institute of Technology, Tokyo, Japan

ABSTRACT

In manufacturing, the monitoring of the fabrication process is crucial in order to be sure that objects are compliant. For nano-objects, most of this monitoring is done manually. In this paper, we propose a method to segment different materials in a manufactured object. The method uses design information which represent the ideal object to manufacture. This representation visually gathers information about materials, shapes and relationships between these shapes. In our segmentation method we choose to encode this information in the tree of shapes to enforce the design characteristics into a real image of the object. To achieve such segmentation, we perform graph cuts on this particular tree structure using additional information such as the position in the design or the order of inclusion of the shapes.

Index Terms— material segmentation, tree of shapes, manufacturing

1. INTRODUCTION

Nano-structured objects are spreading across many different fields of industry to create high performance materials such as is the case for semiconductor, pharmaceutical, cosmetics among others. These objects requires numerous complex steps to be produced. Thus, a monitoring of the different dimensions of the object is needed through these steps to ensure the correct characteristics of the final object. Currently, most of the measurements on these objects are done manually as no software or algorithm is efficient and versatile enough for the early stages of the research and development of such technologies. For these measures, we designed a pipeline as shown in Figure 1. The object detection allows to gather a bounding box around each object. Then the segmentation computes the area covered by each material in each object. Finally, the measure part matches on the segmentation the measurements as expected. In this paper we will cover the segmentation part.

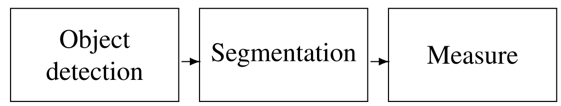

Fig. 1: Complete pipeline for the measure of nano-objects.

From our knowledge, the segmentation based on an image design is not covered by the literature. The characterization of nanomaterials can use imaging techniques such as Transmission Electron Microscopy (TEM). Several classical techniques have been used to segment TEM images. Among them, local or global threshold [1, 2, 3], graph cut [4] and watershed [5, 6, 7, 8], are often used thanks to hight contrast and Signal to Noise Ratio. Recent works used CNN [9, 10]. These works are related to the detection or recognition of particules in powder [1, 2, 6], viruses [11, 10], axons or synapses [4, 9] or Chromatin and DNA [7].

In order to help in the segmentation, designs of the desired objects are available and represent visually the ideal shape of the object in false colors. Each different color symbolize different materials in the real object as shown in Figure 2. From this design, we aim to perform segmentation by materials to help the monitoring of the fabrication. With the simplicity of the design compared to a real image, we chose a more symbolic representation based on trees to be able to add complementary information on the materials. This representation is the tree of shapes.

In this paper, we present first the tree of shapes and its advantages for our problematic. Then, in a second time, we explain the framework we designed in order to segment real images by using a design as guidance. Finally, we discuss the results and finally we conclude.

2. TREE OF SHAPES

The tree of shapes is a representation of the different connected components corresponding to upper and lower levellines of an image ordered in a tree. It was proposed to facilitate the resolution of problems in mathematical morphology as maxima and minima are computed simultaneously [12].

By its construction, the tree of shapes allows us to get a

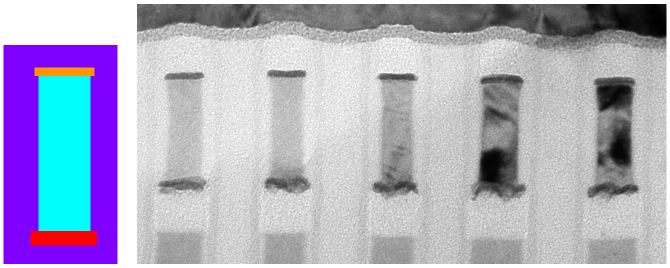

(a) Example of a design

(b) Corresponding manufactured objects

Fig. 2: Example of fabricated objects and its design image. It is some memories pictured in Bright Field

hierarchy between the different materials in the design. As the real object can be assimilated to a noisy, elastically deformed and blurry version of the design, the global structure of both trees is similar and the topology is preserved. This representation presents two main advantages for us [13]. It is invariant to illumination changes which is interesting as acquisition conditions of the objects may vary. Also, as it is constructed with different thresholds the localization of the edges it not shifted when performing filtering of the tree.

3. TREE-CUT

We developed a first approach of segmentation based similar to a 1-nearest neighbor by assigning each node of the object to the closest one from the design in term of similarity of grey-level. This simple approach demonstrates good capabilities but were lacking of regularization.

The objective of tree of shapes cut is to match each node of the object with a node of the tree of shape of the design. We used a segmentation approach by considering each node from the design as a label and thus, labeling the tree of the object with these labels. This assumption allows to gather additional information about the labels. First, it needs to have a given grey-level associated to it which is an approximate mean intensity of the region in the image. The precision of this value does not matter, we want an order between grey-levels. In a second time, we review the regularization in order to be more consistent with our problematic. Finally, we add a second term with the grey-level in order to get more robustness by adding the position in the image.

3.1. General framework

Considering $T = (V, C)$, a tree of shapes with a set of vertex V and a set of links C. We can define T_{design} the tree of shapes of the design and T_{img} the tree of shapes of the object. T_{design} defines the set of labels for the segmentation.

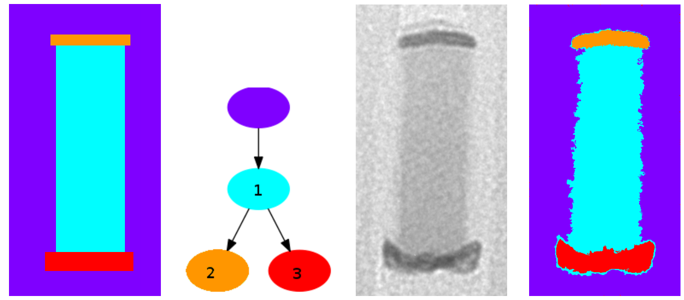

(a) Example of a design

(b) Corresponding Tree of shapes

(c) An example object

(d) The segmentation result

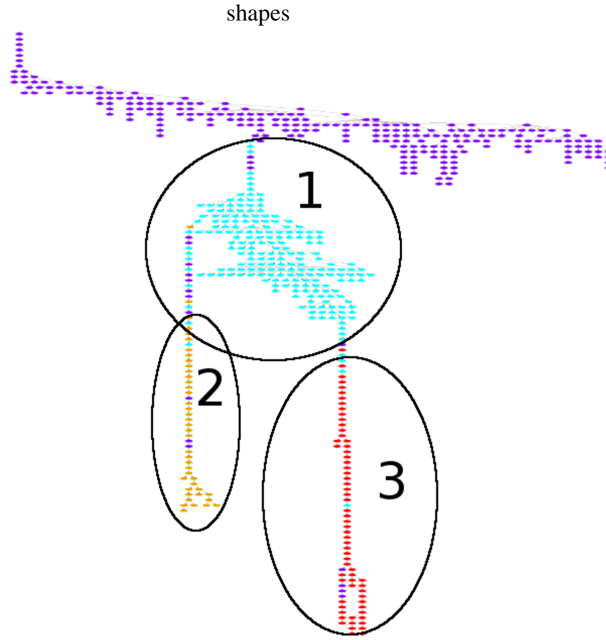

(e) A simplified tree of shapes of a real object fabricated from the design

Fig. 3: Example of similarity between tree of shapes of design and real object.

Each node of this tree has an information about the average expected grey-level. We search to minimize:

$$E(V) = \sum_{\substack{i \in T_{design} \\ j \in T_{img}}} D_{Gi}(V_j) + \sum_{\substack{i \in T_{img} \\ j \in N_i}} R_{ij}(V_i, V_j) \tag{1}$$

with D the data fidelity term, R the regularization term, and N_i the set of nodes that are either $father$ or $child$ of i. In a first time we defined:

$$D_{Gi}(V_j) = \|G_{V_i} - I_j\|_2 \tag{2}$$

$$R_{ij}(V_i, V_j) = \delta(L_{V_i}, L_{V_j}) \tag{3}$$

with G_{V_i} corresponding to the grey-level of the node V_i, L_x corresponding to the node of T_{design} with the same label as x.

In the context of graph cut, minimizing this energy is equivalent to find the min cut in the tree thus, computing the max flow [14].

3.2. Regularization adapted to tree of shapes

The current model used for the regularization is the Potts model adapted to trees. It has the advantage to penalize neighboring nodes. Nonetheless, it penalizes nodes in the same way as they are close or not in the tree of shapes of the design. But in our case, we do not want to mix two regions that are similar in term of grey-levels but far in the tree hierarchy. For example, in Fig 3, considering the region two (orange), if we observed region three (red) labels in it, they will be penalized because they come from a two-distance region. On the other hand, labels from neighboring regions such as region one (cyan) will be less penalized.

In order to still have guaranties in the graph cut in the multi-label case, the new regularization function we want to use has to be a distance or at least a semi distance. For this purpose, we propose to modified the Potts model and replace it to the shortest path between labels as described in equation 4 which satisfies the previous constraint [15] on the tree of shapes.

$$R_{ij}(V_i, V_j) = \min_{\forall P \in T_{design}} \sum_{i=L_{V_i}}^{L_{V_j}} f(C_{i,i+1}) \tag{4}$$

with P a path $P = (C_1, C_2, ..., C_n)$ (where $C_1 = L_{V_i}$ and $C_2 = L_{V_j}$) and $f(C_{i,i+1}) = 1 \; \forall C \in T_{design}$

3.3. Position cost

The data fidelity term we used in our proposition of this general framework is rather simple but we can enhance it by including additional terms. Using only grey-levels information does not give enough robustness because of the important variation of grey-levels in a same material. To increase the use of a priori information present in the design, we chose to use the position information. In this purpose, we resized the design to the same size as the object to have comparable images.

$$D_{Pi}(V_j) = |L_j \cap V_j \setminus L_j \cup V_j| \tag{5}$$

where $|A|$ is the number of elements of the set A and $A \setminus B$ is the complementary of A in the set B.

This new term corresponds to the number of pixels of the current node of the tree of shapes that do not overlap with the corresponding label in the design. Thus, the final data fidelity term D_i is :

$$D_i(V_j) = D_{Gi}(V_j) + \lambda D_{Pi}(v_j) \tag{6}$$

We add a normalization term λ to be able to give more importance to one term or another. In our experiences, we want to give the same importance to grey-level and to position. So, we normalized the position term by the area of the node as described in equation 7 and thus, adapt automatically the lambda to match with the average of the grey-level term.

$$D_{Pi}(V_j) = \frac{|L_j \cap V_j \setminus L_j \cup V_j|}{|V_j|} \tag{7}$$

4. EXPERIMENTS AND RESULTS

For the experiments, we have 2 data sets available. The first one contains objects as show in figure 2, it contains 28 objects. It is parts of memory objects imaged with Transmission Electron Microscopy. On this data, the main challenge is the variability of material 1 (see Figure 3) as some darker pixels appears in the material which is clear that a thresholding approach will not be satisfactory. The second one contains confidential data. It has also three materials and 32 objects. For this data set, the problematic are a low contrast between material 1 and material 2 and a thin segmentation of the material 1 at some places.

We compared our approach against two classical approaches which are the graph cut (GC) and the watershed segmentation. For the graph cut, we select the labels according to the different grey-levels in the design. For the watershed, we computed the ultimate erosion for each label to obtain the seeds. We also compared with an improved version of the graph cut which uses the position in the design as an additional term for the fidelity to the data. Finally, we also proposed a method using the tree of shapes by matching each node of the image to the closest one from the design in term of grey-level intensity.

Table 1: Comparative results of the data set 1 with Dice Index

	GC	Watershed	GC Position	Tree cut
Background	0.50	0.71	0.48	0.79
Material 1	0.09	0.73	0.12	0.68
Material 2	0.46	0.82	0.59	0.90
Material 3	0.72	0.91	0.80	0.95
Mean	0.44	0.79	0.52	0.83

Table 2: Comparative results of the data set 2 with Dice Index

	GC	Watershed	GC Position	Tree cut
Background	0.87	0.91	0.93	0.92
Material 1	0.73	0.24	0.71	0.73
Material 2	0.22	0.51	0.29	0.64
Material 3	0.76	0.86	0.89	0.93
Mean	0.68	0.63	0.70	0.81

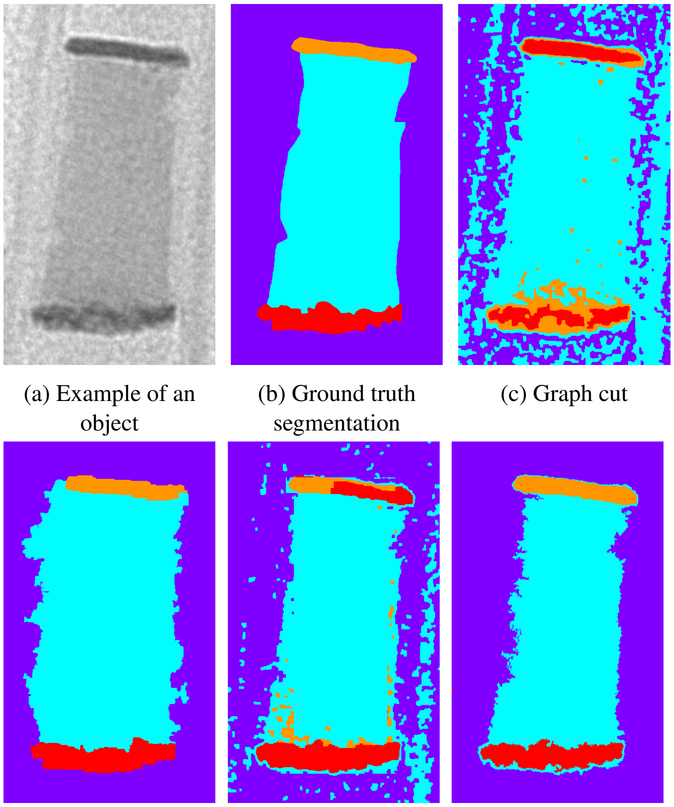

(a) Example of an object (b) Ground truth segmentation (c) Graph cut (d) Watershed (e) Graph cut using position (f) Proposed method

Fig. 4: Comparative results on a simple object from the data set 1.

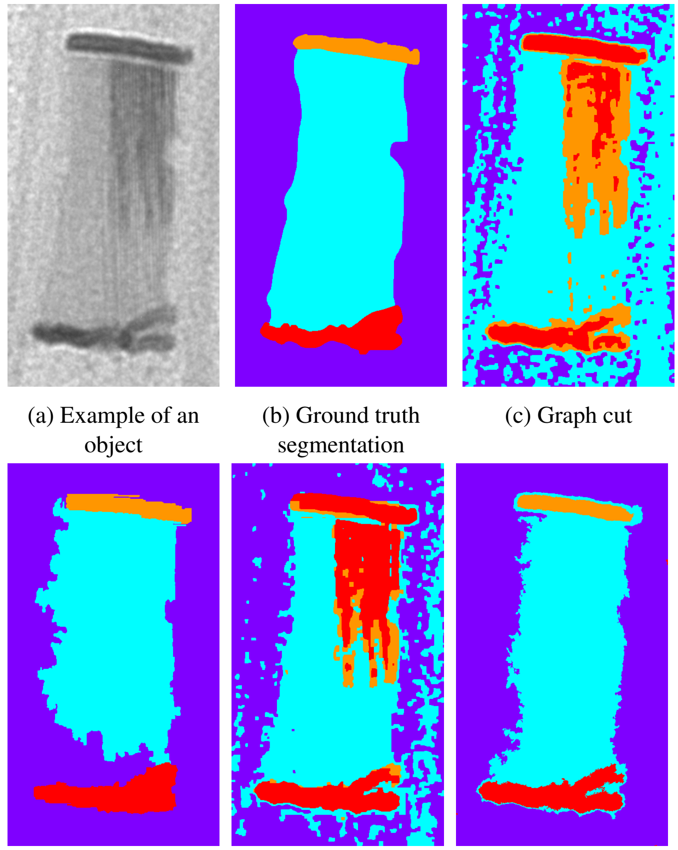

(a) Example of an object (b) Ground truth segmentation (c) Graph cut (d) Watershed (e) Graph cut using position (f) Proposed method

Fig. 5: Comparative results on a difficult object from the data set 1.

On the example shown in Figure 4, we can see that the graph cut approach have difficulties because the materials contrast but the watershed performs way better except for the material one (cyan). On a more difficult example as shown in Figure 5, the watershed begins to show difficulties to get the correct segmentation. The discontinuities of the segmentation of our method are caused by the noise in the image and the structure of the tree of shapes. But in practice, they do not pose to much issues for the measurements. Finally, in table 1 and 2 we can see the different results of each method on both data sets by comparing them with Dice index, which means the closer to 1, the better. On both data sets, material one and two are difficult because of their contrast or because they are similar to another material, and that overall our proposition performs better.

5. CONCLUSION

Our proposed technique takes advantage of the structure of the tree of shapes to perform segmentation. This allows to be robust to the changes of illumination across the data set both inter and intra image. Secondly, edges are not moved during the matching thanks to these properties. Nonetheless, we saw that these different thresholds create some artifacts in the resulting segmentation by including pixels surrounding an inner region.

The use of the framework is also convenient as it allows to leverage the possibility for the tree of shapes to contain numerous attributes about the nodes. We saw that using a second term for the data fidelity helps to deal with outlier regions. The regularization in the framework is also a really strong tool to obtain more homogeneous regions.

In conclusion, we observed that the results are compliant with the design definition but some artifacts remain. For the future work, we think that a better regularization would help for this aspect because the final segmentation should be connected into a single component for each label. Finally, it could be interesting to build the tree of shapes from other attributes than grey-level as the blur in the images tends to create leaks in the segmentation.

6. REFERENCES

[1] Wenhao Yin, Rong Huang, Ruijuan Qi, and Chungang Duan, "Extraction of structural and chemical information from high angle annular dark-field image by an improved peaks finding method," *Microscopy Research and Technique*, vol. 79, no. 9, pp. 820–826, 2016.

[2] Lionel Cervera Gontard, Dogan Ozkaya, and Rafal E. Dunin-Borkowski, "A simple algorithm for measuring particle size distributions on an uneven background from tem images," *Ultramicroscopy*, vol. 111, no. 2, pp. 101 – 106, 2011.

[3] Soleiman Bourrous, Quentin Ribeyre, Laura Lintis, Jérôme Yon, Sébastien Bau, Dominique Thomas, Cécile Vallières, and François-Xavier Ouf, "A semi-automatic analysis tool for the determination of primary particle size, overlap coefficient and specific surface area of nanoparticles aggregates," *Journal of Aerosol Science*, vol. 126, pp. 122 – 132, Dec. 2018.

[4] Nhat Vu and BS Manjunath, "Graph cut segmentation of neuronal structures from transmission electron micrographs," in *2008 15th IEEE International Conference on Image Processing*. IEEE, 2008, pp. 725–728.

[5] Yue Wu, Wen Wang, Fang Zhang, Zhitao Xiao, Jun Wu, and Lei Geng, "Nanoparticle size measurement method based on improved watershed segmentation," in *Proceedings of the 2018 International Conference on Electronics and Electrical Engineering Technology*. ACM, 2018, pp. 232–237.

[6] Pieter-Jan De Temmerman, Eveline Verleysen, Jeroen Lammertyn, and Jan Mast, "Semi-automatic size measurement of primary particles in aggregated nanomaterials by transmission electron microscopy," *Powder Technology*, vol. 261, pp. 191 – 200, 2014.

[7] Yue Li, Eric Roth, Vasundhara Agrawal, Adam Eshein, Jane Fredrick, Luay Almassalha, Anne Shim, Reiner Bleher, Vinayak P. Dravid, and Vadim Backman, "Quantifying three-dimensional chromatin organization utilizing scanning transmission electron microscopy: Chromstem," *bioRxiv*, 2019.

[8] Karel Štěpka, Martin Maška, Jakub Jozef Pálenik, Vendula Pospíchalová, Anna Kotrbová, Ladislav Ilkovics, Dobromila Klemová, Aleš Hampl, Vítězslav Bryja, and Pavel Matula, "Automatic detection and segmentation of exosomes in transmission electron microscopy," in *European Conference on Computer Vision*. Springer, 2016, pp. 318–325.

[9] Aldo Zaimi, Maxime Wabartha, Victor Herman, Pierre-Louis Antonsanti, Christian S. Perone, and Julien Cohen-Adad, "Axondeepseg: automatic axon and myelin segmentation from microscopy data using convolutional neural networks," *Scientific Reports*, vol. 8, no. 1, pp. 3816, 2018.

[10] Damian J. Matuszewski and Ida-Maria Sintorn, "Reducing the u-net size for practical scenarios: Virus recognition in electron microscopy images," *Computer Methods and Programs in Biomedicine*, vol. 178, pp. 31 – 39, 2019.

[11] G. KYLBERG, M. UPPSTRM, K.-O. HEDLUND, G. BORGEFORS, and I.-M. SINTORN, "Segmentation of virus particle candidates in transmission electron microscopy images," *Journal of Microscopy*, vol. 245, no. 2, pp. 140–147, 2012.

[12] P. Monasse and F. Guichard, "Fast computation of a contrast-invariant image representation," *IEEE Transactions on Image Processing*, vol. 9, no. 5, pp. 860–872, May 2000.

[13] Edwin Carlinet, *A Tree of shapes for multivariate images*, Ph.D. thesis, 2015.

[14] Yuri Boykov and Vladimir Kolmogorov, "An experimental comparison of min-cut/max-flow algorithms for energy minimization in vision," *IEEE Transactions on Pattern Analysis & Machine Intelligence*, , no. 9, pp. 1124–1137, 2004.

[15] Thierry Géraud, Yongchao Xu, Edwin Carlinet, and Nicolas Boutry, "Introducing the dahu pseudo-distance," in *International Symposium on Mathematical Morphology and Its Applications to Signal and Image Processing*. Springer, 2017, pp. 55–67.